

Journal Pre-proofs



Knocking out FAM20C in pre-osteoblasts leads to up-regulation of osteoclast differentiation to affect long bone development

Lili Jiang, Xinpeng Liu, Lixue Liu, Lide Su, Zeyu Lu, Hong Zhang, Yuyao Guo, Wenxuan Zhang, Shujian Zhang, Wenxia Xu, Jiahui Zhang, Kai Zhang, Yuanbo Zhan, Xiaohua Xie, Runhang Li, Xinhe Dong, Han Jin, Bin Zhang, Ying Li

PII: S0378-1119(24)00277-4
DOI: <https://doi.org/10.1016/j.gene.2024.148396>
Reference: GENE 148396

To appear in: *Gene Gene*

Received Date: 13 November 2023
Revised Date: 23 February 2024
Accepted Date: 18 March 2024

Please cite this article as: L. Jiang, X. Liu, L. Liu, L. Su, Z. Lu, H. Zhang, Y. Guo, W. Zhang, S. Zhang, W. Xu, J. Zhang, K. Zhang, Y. Zhan, X. Xie, R. Li, X. Dong, H. Jin, B. Zhang, Y. Li, Knocking out FAM20C in pre-osteoblasts leads to up-regulation of osteoclast differentiation to affect long bone development, *Gene Gene* (2024), doi: <https://doi.org/10.1016/j.gene.2024.148396>

This is a PDF file of an article that has undergone enhancements after acceptance, such as the addition of a cover page and metadata, and formatting for readability, but it is not yet the definitive version of record. This version will undergo additional copyediting, typesetting and review before it is published in its final form, but we are providing this version to give early visibility of the article. Please note that, during the production process, errors may be discovered which could affect the content, and all legal disclaimers that apply to the journal pertain.

© 2024 The Author(s). Published by Elsevier B.V.

Knocking out FAM20C in pre-osteoblasts leads to up-regulation of osteoclast differentiation to affect long bone development

Lili Jiang^a, Xinpeng Liu^b, Lixue Liu^a, Lide Su^c, Zeyu Lu^a, Hong Zhang^d, Yuyao Guo^a, Wenxuan Zhang^a, Shujian Zhang^a, Wenxia Xu^a, Jiahui Zhang^a, Kai Zhang^a, Yuanbo Zhan^e, Xiaohua Xie^e, Runhang Li^d, Xinhe Dong^d, Han Jin^{a***}, Bin Zhang^{a,f**}, Ying Li^{a*}

^a*Heilongjiang Provincial Key Laboratory of Hard Tissue Development and Regeneration, The Second Affiliated Hospital of Harbin Medical University, Harbin, China*

^b*Department of Oral and Maxillofacial Surgery, Stomatological Hospital, Southern Medical University (Guangdong Provincial Stomatological Hospital), Guangzhou, Guangdong, China*

^c*Department of Cardiovascular Surgery, Xiang'an Hospital of Xiamen University, School of Medicine, Xiamen University, Xiamen, 361005, Fujian, China.*

^d*School of Stomatology, The First Affiliated Hospital of Harbin Medical University, Harbin, China*

^e*The Second Affiliated Hospital of Harbin Medical University, Harbin, China*

^f*Heilongjiang Academy of Medical Sciences, Harbin, Heilongjiang, China*

*Corresponding author at: The Second Affiliated Hospital of Harbin Medical University, 246 Xuefu Road, Harbin, Heilongjiang, 150001, China.

E-mail address: liying@hrbmu.edu.cn (Y. Li)

**Corresponding author at: The Second Affiliated Hospital of Harbin Medical University, 246 Xuefu Road, Harbin, Heilongjiang, 150001, China.

E-mail address: zhangbin@hrbmu.edu.cn (B. Zhang)

***Corresponding author at: The Second Affiliated Hospital of Harbin Medical University, 246 Xuefu Road, Harbin, Heilongjiang, 150001, China.

E-mail address: jinhan@hrbmu.edu.cn (H. Jin)

Highlights

- FAM20C phosphorylates regulatory proteins involved in bone development
- A novel *Osx*-Cre; *FAM20C*^{flox/flox} knockout (oKO) mouse model is established
- oKO has lower bone mineralization, along with greater hypertrophic cartilage
- oKO has up-regulation of osteoclast differentiation genes *Sirpb1a-c* and *Mapk13*
- Osteogenesis-related genes *Osx*, *Alp*, *Ocn*, *Mepe*, and *Col2* are downregulated in oKO

Abstract

Family with sequence similarity 20 member C (FAM20C) is a Golgi casein kinase that phosphorylates extracellularly-secreted regulatory proteins involved in bone development and mineralization, but its specific role in bone development is still largely unknown. In this study, to examine the specific mechanisms that FAM20C influences bone development, we cross-bred *Osx*-Cre with *FAM20C*^{flox/flox} mice to establish a *Osx*-Cre; *FAM20C*^{flox/flox} knockout (oKO) mouse model; FAM20C was KO in pre-osteoblasts. oKO development was examined at 1-10 weeks, in which compared to control *FAM20C*^{flox/flox}, they had lower body weights and bone tissue mineralization. Furthermore, oKO had lower bone volume fractions, thickness, and trabecular numbers, along with higher degrees of trabecular separation. These mice also had decreased femoral metaphyseal cartilage proliferation layer, along with thickened hypertrophic layer and increased apoptotic cell counts. Transcriptomic analysis found that differentially-expressed genes in oKO were concentrated in the osteoclast differentiation pathway, in line with increased osteoclast presence. Additionally, up-

regulation of osteoclast-related, and down-regulation of osteogenesis-related genes, were identified, in which the most up-regulated genes were signal regulatory protein β -1 family (Sirpb1a-c) and mitogen-activated protein kinase 13. Overall, FAM20C KO in pre-osteoblasts leads to abnormal long bone development, likely due to subsequent up-regulation of osteoclast differentiation-associated genes.

Key words: FAM20C; osteoclast differentiation; bone development; conditional knockout; SIRPB1

FAM20C	Family with sequence similarity 20 member C
SCPPs	secretory calcium-binding phosphoprotein
SIBLING	small integrin-binding ligand n-linked glycoprotein families
KO	knockout
Mapk13	mitogen-activated protein kinase 13
TRAP	tartrate-resistant acid phosphatase
TUNEL	transferase dUTP nick end labeling
Ctsk	Cathepsin K
Mmp9	matrix metalloproteinase protein 9
Nfatc1	nuclear factor of activated T-cells, cytoplasmic 1
Osx	osteogenesis-related genes Sp7
Alp	alkaline phosphatase
Mepe	matrix extracellular phosphoglycoprotein

Col2	collagen type 2
SIRPs	signal-regulatory protein
BAO	bone-associated osteoclast
IGFBP3	insulin-like growth factor-binding protein 3

1. Introduction

Bone tissue serves a variety of functions within organisms, such as mechanical support, locomotion, blood cell production, mineral storage, and endocrine regulation (van Gestel and Carmeliet, 2021). Its development is a complex, delicately-balanced process, involving bone formation by osteoblasts, and resorption by osteoclasts; other cell types, such as chondrocytes and immune cells, are also involved (Salhotra et al., 2020). Disruption of this delicate balance serves as the underlying basis behind numerous bone diseases (Kim et al., 2020). Therefore, the regulation of bone development has been a topic of much research, as it may have significant therapeutic implications for treating bone diseases and aging-related degeneration.

Family with sequence similarity 20 member C (FAM20C) is a Golgi casein kinase, whose activation involves homodimer formation with another FAM20C molecule, or a heterodimer with FAM20A, which is more effective, owing to FAM20A possessing an optimized hydrophobic surface, comprising of Ile214A, Ile255A, and Leu365A (Xu et al., 2021). It phosphorylates over 100 secretion-related proteins, preferentially those with the S-x-E/pS motif. These phosphorylated proteins have been implicated in cardiovascular and neurovascular disease pathogenesis (Xu et al., 2021), as well as the regulation of coagulation pathways, such as by Da et al., who found that von Willebrand factor, a key platelet aggregation factor, was one of the many phosphorylation targets of FAM20C (Da et al., 2019). FAM20C-phosphorylated proteins have also been linked to different cancers, one of which is bone morphogenetic protein 4, whose phosphorylation has been observed to promote breast cancer metastasis to bone (Zuo et al., 2021).

A prominent biological process involving FAM20C is bone development and mineralization, as demonstrated by mutations on this gene resulting in Raine syndrome in humans, manifesting as diffuse periosteal osteosclerosis, hypophosphatemic osteomalacia, tooth and bone dysplasia, and craniosynostosis, which could be fatal in severe cases. Furthermore, multiple *in vitro* studies have shown that FAM20C directly regulates osteoblast behavior (Liu et al., 2017a; Geng et al., 2022); one study was previously carried out by our group, in which we observed that knocking out (KO) FAM20C in osteoblasts, resulted in

lowered cell migration, due to reduced calpastatin/calpain proteolysis system activity (Liu et al., 2023). Additionally, FAM20C has been identified as phosphorylating target proteins involved in bone development and mineralization, such as members of the secretory calcium-binding phosphoprotein (SCPPs), fibroblast growth factor 23 (FGF23) and small integrin-binding ligand n-linked glycoprotein families (SIBLING), all of which are involved in biomineralization. In particular, SIBLING proteins include dentin matrix protein (DMP1), bone sialoprotein (BSP), osteopontin (OPN), extracellular phosphoglycoprotein matrix (MEPE) and dentine sialophosphoprotein (DSPP), which have all been implicated in the precipitation of calcium phosphate to form hydroxyapatite in bone and teeth (Palma-Lara et al., 2021).

However, osteoblast-specific KO has not been fully established in animal models; indeed, one of the few documented involved crossbreeding Sox2 (sex determining region Y-box 2)-Cre with FAM20C^{flox/flox} to establish a Sox2-Cre; FAM20C^{flox/flox} mouse model, which recapitulated the symptoms of amelogenesis imperfecta (Liu et al., 2020). However, with respect to bone growth and development, it is difficult to fully tease out the exact effects of FAM20C KO. This is due to Sox2-Cre recombinase being expressed in a variety of tissues in these KO models (Zhang et al., 2023), as well as the large number of downstream substrates of FAM20C (Wang, 2012; Liu et al., 2017b; Zhang et al., 2019).

In this study, we aimed to shed light on the specific effects of FAM20C on bone development, via establishing the osterix (osteoblast-specific factor; Osx)-Cre; FAM20C^{flox/flox} (oKO) mouse model to conditionally knockout FAM20C in pre-osteoblasts (Yu et al., 2021). Specific FAM20C KO was confirmed within the femur, and its effects and related mechanisms for bone development were evaluated.

2. Materials and Methods

2.1. Construction of the oKO mouse model and obtaining bone tissue samples

oKO mice were obtained by cross-breeding FAM20C^{flox/flox} (Texas A&M University College of Dentistry, USA) with Osx-Cre (Biocytogen, China) mice; the flox site is inserted at exons 6-9 of the Fam20c gene. This insertion site is highly conserved among species, and in humans is where Fam20c mutations occur. Their genotype was confirmed by mouse tail DNA (Tiangen, YDP304) extraction and PCR, using a 3-primer strategy. There, primers FAM20C-a and -b amplified a 400 bp band, representing the floxed segment, while FAM20C-a and -c amplified a 500 bp band, representing the wild-type FAM20C allele (Table S1). FAM20C^{flox/flox} was represented by a single 400 bp band, while heterozygosity for one of the loxP sites was indicated by a double band of 400 and 500 bp, and wild-type by a single 500 bp band (Fig. S1A). The presence of Osx-Cre was indicated by the presence of a single 445 bp band, which was not present among wild-type (Fig. S1B). Therefore, oKO was indicated by the presence of a single 400 bp band (Lane 4; Fig. S1A), and a single 445 bp band (Lane 4; Fig. S1B). Control mice comprised of littermates of oKO mice, with only FAM20C^{flox/flox}; under PCR, they were indicated by the presence of a single 400 bp band

(Lane 7; Fig. S1A-B). No significant differences were found between male and female mice for both mouse groups.

To obtain femur samples, mice at 1, 2, 3, or 4 weeks were sacrificed, in which they were internally-fixed after anesthesia. The femur was bluntly dissected and fixed in 4% paraformaldehyde for 48 h, then decalcified using 15% EDTA (pH 7.2-7.4). Decalcification endpoint was identified by bone puncture, without any resistance. After decalcification, the bone tissue was dehydrated, according to the following procedure: first by increasing grades of alcohol from 70%, 80%, 85%, then, respectively, 2 changes of 95% and 100% alcohol, as well as 3 changes of xylene. Femurs were then paraffin-embedded, and 3 μm sections were obtained. All animal procedures were approved by the Ethics Committee of Second Affiliated Hospital of Harbin Medical University (REB #: SYDW2021-079), and were carried out in accordance with the Guide for the Care and Use of Laboratory Animals (NIH, 8th Edition, 2011).

2.2. X-ray and Micro-CT analysis of bone tissue

Before anesthetization and sacrifice of mice at 1, 2, 3, and 4-weeks-old, both oKO and control mice were placed in the same field of view for the small animal X-ray machine (Faxintron). X-rays were taken to compare bone growth between both groups for the entire body. After removal and fixation of the sternum and femur for 24 hours, a stereomicroscope was used to aid in further removing the superficial fascia, muscles, and other tissues from the bones. X-rays were then taken, involving control and oKO bones, at the same positions, time points, fields of view, and exposure times, to observe local bone tissue morphologies. To perform micro-CT (Scanco), femurs were scanned using a 6.7 mm aperture, and each layer, with high precision of 6 μm , was selected for 3-dimensional reconstruction, for analyzing various femoral tissue parameters.

2.3. Histological staining

The general structure of the femur was depicted using hematoxylin & eosin (H&E) staining (Solarbio, G1120). Briefly, tissue sections were deparaffinated by baking them at 65°C for 30 min, hydrated to water, stained with hematoxylin for 1 min and eosin for 2 min, then dehydrated and mounted with neutral gum.

Furthermore, at the femoral growth plate, chondrocytes were identified using safranin-O-fast green staining (Solarbio, G371), owing to safranin O being a basic dye that is able to electrostatically bind to the anionic sulphate and carboxyl groups present in cartilage glycosaminoglycans, proteoglycans, and collagens, as demonstrated by Ruhl et al. (Ruhl and Beier, 2019), leading to the chondrocytes being stained red. In brief, tissue sections were stained with Weigert's hematoxylin for 3 min, followed by acid differentiation for 15 s, washing with distilled water for 10 min, staining with fast green solution for 5 min, washing with a weakly acidic solution for 10-15 s, and safranin-O solution staining for 5 min.

Osteoclasts were stained using the AS kit (Servocebio, G1050), as TRAP is a specific marker for those cells (Hayman, 2008). For this procedure, tissue sections were incubated in distilled water, at 37°C, for 2 h, then incubated in TRAP staining solution at 37°C for 30 min. Nuclei were counter-stained with methyl green for 5 min.

Apoptotic cells at the femoral growth plate were identified using terminal deoxynucleotidyl transferase dUTP nick end labeling (TUNEL; Beyotime, C1091). For this purpose, tissue sections were incubated with 20 µg/mL proteinase K for 20 min at 37°C, labelled with biotin-labelled dUTP at 37°C for 1 h, followed by streptavidin-horseradish peroxidase for 30 min at room temperature. Afterwards, color development was obtained by 3'3'-diaminobenzidine (DAB) chromogenic solution.

Immunohistochemical staining for FAM20C (Proteintech, 25395-1-AP; 1:200) and Caspase3 (Abmart, TA6311; 1:400) was also performed, as follows: tissue sections were deparaffinated, treated with proteinase K and H₂O₂, then incubated with primary antibodies in darkness, for 1.5-2 h, at 37°C. Afterwards, femur sections were incubated with horseradish-conjugated secondary antibodies at room temperature for 30 min, and visualized using DAB substrate. Methyl green was used to counterstain nuclei.

2.4. Bone tissue RNA extraction, RT-qPCR, and transcriptomic analysis

RNA was extracted from the femurs of 4-week-old mice with RNAiso Plus reagent (Takara, 9108), after they were flash-frozen with liquid nitrogen and ground with mortar and pestle. One mg RNA was used as the template for reverse transcription, using a 2-step method (Takara, RR047A). Once cDNA was obtained, qPCR was carried out, using SYBR Green master mix (Takara, RR820A) under the following program: 95°C for 2 min, followed by 95°C for 5 s, 60°C for 10 s, and 72°C for 20 s, for 40 cycles. Gene expression was quantified using the $2^{-\Delta\Delta C_t}$ method, and normalized to the house-keeping gene GAPDH. The primers used are shown in Table S1.

To carry out transcriptomic analysis, total RNA from 4-week-old mouse femurs (3/group) were extracted, purified, and mRNA captured, using Dynabeads Oligo (dT) (Cat # 25-61005, Thermo Fisher, USA) with affinity for poly-adenylic acid, in 2 rounds of purification. mRNA was fragmented under temperature control, and reverse-transcribed into cDNA (Takara, RR047A). After editing, cDNA was amplified to obtain the single-stranded DNA library, and sequencing data was recorded using paired-end next-generation sequencing (Illumina NovaSeq 6000, LC Bio Technology Co., Ltd., Hangzhou, China), with reads 150 bp in length (PE150). This data was then filtered for high-quality ones, based on $|\log_2(FC)| \geq 1$, $p < 0.05$, and compared to existing mouse gene libraries to quantify gene expression levels, as well as for conducting differential and enrichment analyses. These differential and enrichment analyses were conducted using the Gene Ontology, as well as Kyoto Encyclopedia of Genes and Genomes (KEGG) databases.

2.5. Statistical analysis

Data were expressed as mean \pm standard deviation. All experiments were performed in triplicate. Analyses were performed using GraphPad Prism software (v. 8.4). Unpaired Student's t-test (2-tailed) was performed for comparisons between 2 groups. $P < 0.05$ were considered statistically significant.

3. Results

3.1. Successful establishment of the oKO mouse model with dysplastic bone tissue

To verify successful crossbreeding of *Osx-Cre* with *FAM20C^{flox/flox}* mice to obtain oKO mice, we first carried out PCR genotyping, in which oKO mice, as shown in Lane 4, a 400 bp and a 445 bp band, representing, respectively, the presence of both *FAM20C^{flox/flox}* (Fig. S1A) and *Osx-Cre* genes (Fig. S1B). By contrast, control mice only had a single 400 bp band, as shown in Lane 7 (Fig. S1A-B). PCR genotyping results were further confirmed by immunohistochemical staining, where oKO was negative for *FAM20C* among pre-osteoblasts in both femur cortical bone and trabeculae, while control had *FAM20C* expression (Fig. S1C), as well as by RT-qPCR, in which oKO mice had significantly lower *FAM20C* mRNA levels, compared to control (Fig. S1D).

To examine the effects of *FAM20C* KO on bone development, mouse body weights were first observed for both groups over a 10-week period, in which oKO had significantly slower weight growth, and a flatter growth curve, from Week 3 onwards. By contrast, the control group had more rapid growth from Week 4, corresponding to puberty (Fig. 1A). Under X-rays, oKO mice, from Weeks 1-4, were also smaller in size (Fig. S2A-B; Fig. 1B), and had shorter limb bones (Fig. S2C; Fig. 1C). oKO limb bones also had a smaller 2nd ossification center, and thus a wider epiphyseal plate area; both the ossification center appearance, and closure of the epiphyseal plate, occurred later versus control (Fig. S2C; Fig. 1C). All of these observations were indicative of slower bone formation and poorer mineralization, which was further supported by rib X-rays (Fig. S2D) and micro-CT of the 4-week-old femur. There, the cortical bone among oKO was thin and discontinuous, and the epiphyseal plate, which normally closes at 4-weeks, was still open (Fig. 1D). Additionally, 3D reconstructions showed that less trabecular formation was present among oKO versus control, at the distal region of the epiphyseal plate (Fig. 1E; Fig. S2E). This lowered trabecular formation was also found, under osteometry, to be present in terms of volume fraction, number of trabeculae, and trabecular bone thickness. Additionally, the separation distance between trabeculae was higher in oKO (Fig. 1F). All these findings thus demonstrate that oKO mice had been successfully established, and that knocking out *FAM20C* in pre-osteoblasts results in defects in bone formation, with respect to growth, mineralization, epiphyseal plate closure, and trabecular formation.

3.2. oKO mice demonstrated growth plate hypertrophy, thickened cartilage layer, and bone dysplasia

In light of slower epiphyseal plate closure and poorer ossification being observed among oKO, we then conducted further histological examinations of the femur tissue to identify possible underlying morphological alterations, starting with H&E staining. We found that at 1-2 weeks, cartilage comprises the majority of the proximal femur, and that the proliferation layer within that cartilage was active. In the control group, proliferating cartilage cells are regularly arranged in cords, while in oKO, they are irregularly-gathered (Fig. S3A). At 3 weeks, the hypertrophy layer of the cartilage thickens, while the proliferation layer remains similar to that of weeks 1-2, among both groups (Fig. S3A). At 4 weeks, the number of chondrocyte layers in the quiescent and proliferative zones of the

epiphyseal cartilage for oKO is smaller than for control. However, oKO has a thicker hypertrophy cartilage layer, both at the epiphyseal growth plate, and at the articular surface, with irregular, polygonal vacuolar chondrocytes possessing unclear nuclei (Fig. 2A).

Based on our observations of the thickened hypertrophy cartilage layer in oKO versus control mice under morphological analysis, we further investigated the chondrocytes in that layer using cell-specific staining, as well as identifying whether apoptosis of these cells occurred. First, safranin O-fast green staining was conducted at the long epiphyseal region for Weeks 1-4 mice, in which from Week 1 onwards, the hypertrophic cartilage layers are thicker, with irregular arrangements, in oKO mice. The chondrocytes in those layers were also irregularly-shaped (Fig. 2B; Fig. S3B). It was also found that a layer of red-stained cartilage matrix, which was not fully mineralized, was present in oKO, while it was mostly absent in the control (Fig. S3B). We then quantified the number of apoptotic cells within the cartilage proliferation and calcification areas of the epiphyseal plate, in which at 4 weeks, greater numbers of apoptotic chondrocytes were present in oKO (Fig. 2C-D). oKO also had greater expression levels for caspase-3, a classical apoptotic marker (Fig. 2E-F). Collectively, these observations thus demonstrate that oKO mice had greater cartilage hypertrophy, with more irregular layers at the epiphyseal plate, as well as greater amounts of non-mineralized matrix, representing bone dysplasia. This greater hypertrophy was also coupled with greater amounts of chondrocyte apoptosis.

3.3. Transcriptome analysis of femur tissue showed up-regulation of osteoclast differentiation-related genes among oKO mice

To investigate the specific underlying molecular mechanisms FAM20C is involved in for long bone growth and development, transcriptome analysis was conducted on 4-week-old mouse femurs. We found that compared to control, oKO had 118 up-, and 149 down-regulated differentially-expressed genes (Fig. 3A-C). Gene functions were found under Gene Ontology enrichment analysis to be involved in multiple biological processes, mostly in relation to cell membrane functioning, as well as extracellular matrix and space (Fig. 3D). Additionally, KEGG analysis indicated that the processes with the most up-regulated genes among oKO was osteoclast differentiation, while the pathway most related to the bone development process was thyroid hormone synthesis (Fig. 3E), which was found to be down-regulated (Fig. S4A). KEGG analysis also found up-regulation of genes related to hematopoietic cell lineages and paracrine pathways (Fig. S4A). The most up-regulated genes in the osteoclast differentiation pathway were *Sirpb1a*, *Sirpb1b*, *Sirpb1c*, *Mapk13*, suppressor of cytokine signaling 3 (*Socs3*), and *Gm9733*, which were marked on the volcano plot in Figure 3C. *Mapk13* up-regulation was further supported by gene set enrichment analysis (GSEA), which found that MAPK, as well as the adaptor protein, DNAX activation protein of 12 kDa (*DAP12*), that interacts with MAPK, were up-regulated among oKO mice (Fig. S4B). Western blot analysis confirmed this observation, in which higher p38 MAPK levels were present among the femurs of 4-week-old oKO mice, compared to control (Fig. S4C). All these analyses thus suggest that FAM20C was involved in bone development via regulating osteoclast differentiation.

3.4. Knocking out FAM20C promotes osteoclast differentiation and suppressing osteogenesis

To confirm our transcriptome analysis finding that FAM20C was associated with osteoclast differentiation, we performed TRAP staining to quantify osteoclasts in mouse femur tissue. At 4 weeks, oKO had significantly more osteoclasts within femoral cancellous bone, with their characteristic multiple nuclei and cytoplasmic extensions (Fig. 4A-B). This finding thus indicates that bone resorption is more active in oKO versus control mice.

We then investigated whether expression level differences in osteoclast-related genes, identified by transcriptome analysis, was present. Using qPCR, we found that expression levels for osteoclast-specific genes Cathepsin K (*Ctsk*), matrix metalloproteinase protein 9 (*Mmp9*), nuclear factor of activated T-cells, cytoplasmic 1 (*Nfatc1*), and *Trap* (Fig. 4C), as well as the osteoclast differentiation-associated genes *Sirpb1a*, *Sirpb1b*, *Sirpb1c*, and *Mapk13* were higher among oKO versus control (Fig. 4D). By contrast, expression levels for osteogenesis-related genes *Sp7* (*Osx*), alkaline phosphatase (*Alp*), osteocalcin (*Ocn*), matrix extracellular phosphoglycoprotein (*Mepe*), and collagen type 2 (*Col2*) were lower among oKO, compared to control (Fig. 4E). All these findings thus indicated that FAM20C KO promoted osteoclast differentiation and functioning, while suppressing osteogenesis-related signaling pathways.

4. Discussion

FAM20C is a highly-conserved Golgi casein kinase, which has far-reaching significance regarding bone development in various organisms (Zhang et al., 2018). It has been documented in multiple studies to specifically recognize the S-x-E/pS motif, enabling it to phosphorylate over 100 secreted phosphoproteins, such as SCPPs and SIBLING, which play important roles in bone development and mineralization (Tagliabracci et al., 2015; Dab et al., 2022). Due to its importance in these processes, numerous *in vivo* animal models have been established, most of which are conditional KO, involving cross-breeding with the likes of *Sox2-Cre* and 3.6 kb *Colla1-Cre* mice, which has yielded skeletal defects (Wang, 2012; Liu et al., 2017b; Zhang et al., 2019). However, the specific role that FAM20C plays in bone development has still not been fully defined. Therefore, in this study, we established the *Osx-Cre; FAM20C^{lox/lox}* mouse model for conditionally deleting FAM20C in pre-osteoblasts. The novelty of our findings are: 1) The first to generate the *Osx-Cre; FAM20C^{lox/lox}* mouse model to KO FAM20C in pre-osteoblasts *in vivo*, 2) Identification of *Sirpb1a-c* and *Mapk13* up-regulation, which promote osteoclast differentiation, in FAM20C KO, coupled with 3) Down-regulation of osteogenesis-related genes *Osx*, *Alp*, *Ocn*, *Mepe*, and *Col2*. Furthermore, we found that compared to *FAM20C^{lox/lox}* control, femur ossification centers appeared later, and poorer whole-body bone tissue mineralization was present. Additionally, intramembranous and cartilage osteogenesis processes were affected to varying degrees (Berendsen and Olsen, 2015). We also observed that some oKO mice possessed variable sternal shapes and femoral osteolysis, which could potentially be due to increased osteoclast activity, though further research is needed to fully elucidate the underlying mechanisms.

In terms of underlying mechanisms, KEGG analysis of bone tissue transcriptomes among 4-week-old mice identified that the most significant difference in pathway activation between oKO and control mice was the osteoclast differentiation pathway, which was higher in the former versus the latter. Indeed, oKO mice had more active osteoclasts and greater amounts of bone resorption, which corresponded to trabecular bone osteometry results, where lowered trabecular formation, in terms of volume fraction, number of trabeculae, and trabecular bone thickness was present. This may be due to pre-osteoblast FAM20C KO affecting subsequent osteoblast-osteoclast interaction, leading to increased osteoclast differentiation and activities. We also found that FAM20C KO directly affected osteoblast function via down-regulating osteoblast-related gene expression. Therefore, the changes in osteoblast and osteoclast activities associated with FAM20C KO is most likely due to FAM20C KO disrupting the dynamic relationship between osteoblasts and osteoclasts. This disruption may be based on alterations in osteoblast juxtacrine and paracrine activities (van Driel and van Leeuwen, 2023), which is supported by KEGG analysis also showing up-regulation of genes that affect paracrine function.

Indeed, pathways involved in osteoclast-osteoblast coupling have been implicated in regulating osteoclast differentiation. These include receptor activator of nuclear factor κ B and its ligand (RANK/RANKL), as well as macrophage colony-stimulating factor and its receptor (M-CSF/c-Fms) (Udagawa et al., 2020; Yao et al., 2021). One such interaction involves signal-regulatory protein (SIRPs), a family of transmembrane glycoprotein secreted by macrophages and monocytes. The main member of this family, SIRPB1, has been found to play a role in the osteoclast differentiation pathway (Barclay and Brown, 2006; Barclay, 2016), via its interaction with triggering receptor expressed on myeloid cells 2 (TREM2), expressed on the surface of monocytes. In fact, SIRPB1, TREM2, and DAP12 have been found to form a complex that regulates calcium movement, and subsequently osteoclast differentiation (Beek et al., 2009; Zou et al., 2010; Sundaram et al., 2017). It is worth noting, though, that the combination of SIRPB1 and DAP12 alone cannot induce osteoclast formation, but it is able to play a synergistic role. Indeed, *Sirpb1*, comprising of 3 subtypes, *Sirpb1a-c*, acts as a “catalytic enzyme” to promote TREM2 and DAP12 combination, and thus catalyzing osteoclast differentiation. SIRPB1 has also been found, when cross-linked with monoclonal antibodies in a mouse model, to trigger SYK and MAPK phosphorylation, both of which promotes macrophage phagocytosis (Hayashi, 2004). These connections between SIRPB1, MAPK, and osteoclast activity were further supported by the finding that bone resorption was inhibited by a polyphenol extract, which was able to lower expression levels for various stimulatory factors, including SIRPB1, as well as calcium levels and MAPK pathway activity. All of this inhibition, in turn, affected *Nfact1* expression, and subsequently reduced osteoclast formation and activity (Graef, 2017). Additionally, studies using the DAP12 KO model found that free SIRPB1 could still impact osteocyte differentiation, via the MAPK pathway, even though there was no substrate for it to “catalyze” (Dietrich, 2000; Tomasello, 2015). Our findings were in line with those previous observations, in that *Sirpb1a-c*, as well as *Mapk13*, were significantly up-regulated after conditional KO of FAM20C in pre-osteoblasts. This up-regulation of SIRPB1 family members thus promotes osteoclast differentiation, via the MAPK pathway, thereby affecting cancellous bone development in long bones.

Besides those newly identified up-regulated *Sirpb1a-c* and *Mapk13* proteins in FAM20C KO which promote osteoclast differentiation, we also identified genes associated with decreased osteoblast differentiation and activity, which subsequently contributed to lowered bone tissue mineralization. More specifically, our observations of down-regulated osteoblast-associated gene expression, such as for osteogenesis-related genes *Osx*, *Alp*, *Ocn*, *Mepe*, and *Col2*, were supported by Liu et al., who also found reduced *Alp* expression, along with *Dmp1*, *Dspp*, and type I collagen a 1 (*Col1a1*) (Liu et al., 2017a), all of which have been linked to defective osteoblast differentiation in FAM20C-deficient osteoblasts *in vitro*. Conversely, Hirose et al. noted that *in vivo* FAM20C overexpression was associated with increased cortical bone formation (Hirose et al., 2020). More recently, a possible underlying mechanism was identified in which FAM20C KO in osteoblasts reduced osteoblast migration, due to lowered calpastatin phosphorylation and calpain activity, leading to the up-regulation of Wnt/ β -catenin signaling proteins (Liu et al., 2023). However, it is worth to emphasize that the basis behind FAM20C effects on osteoblast/osteoclast function may involve more complex interactions among signaling pathways, rather than mere phosphorylation of substrates by FAM20C, as attempts to rescue defective osteoblast differentiation in FAM20C-deficient cells with phosphorylated proteins extracted from normal bone failed (Liu et al., 2017a). By contrast, transgenic mice with *Dspp* overexpression was able to alleviate osteoblast differentiation defects present in a *Dmp1* KO mouse model, suggesting that these defects could be counteracted if it was downstream of FAM20C (Gibson et al., 2013). Nevertheless, future studies should be conducted to elucidate the full effects of FAM20C KO and map out the affected interactions with other signaling pathways.

FAM20C has also been documented to be the downstream mediator of mechanoreceptors involved in regulating the conversion of H- (juvenile bone) to L-type blood vessels (adult bone), in response to weight gain during puberty. In fact, in response to mechanoreceptor activity, FAM20C regulates DMP1 secretion, which in turn is associated with the termination of long bone development (Dzamikova et al., 2022). We found that among 4-week-old mice, those with FAM20C KO did not experience puberty-associated rapid weight growth, yielding a flatter growth curve. These mice also had impaired mechanosensory conduction and ossification, along with greater numbers of multinucleated osteoclasts and bone resorption.

Our KEGG analyses identified that genes associated with hematopoietic cell lineages and paracrine pathways were up-regulated among oKO mice, which could be owed to hematopoietic stem cells being one of the sources for osteoclasts, in turn serving as the possible basis for FAM20C KO leading to increased resorptive bone-associated osteoclast (BAO) cells. Recent studies have documented that osteoclasts could be divided into 2 types, based on their functions: 1) vascular-associated, which induces blood vessel ingrowth and promotes cartilage ossification, and 2) resorptive BAO, which are located around trabecular bone and promotes bone resorption (Romeo et al., 2019). Indeed, poorer trabecular bone formation was present among oKO mice, which is in line with increased BAO. Puberty also promoted the thyroid hormone-induced *Osx* signaling pathway to transform cartilage into osteoblasts. This association between thyroid hormone and osteoblast development was

supported by our KEGG analysis, in which oKO mice had down-regulated expression for thyroid hormone formation-associated genes. This down-regulation subsequently affected cartilage ossification (Xing et al., 2019), which, along with thickening of the hypertrophic cartilage layer and abnormal cancellous bone resorption, contributed to abnormal long bone development in these mice. The abnormally-thickened hypertrophic cartilage layer and damaged ossification processes at the epiphyseal plate among oKO mice may also be owed to differences in osteoclast-secreted exosomal cytokines affecting cartilage ossification (Dai, 2020). In this study, we found that insulin-like growth factor-binding protein 3 (IGFBP3) expression was up-regulated in the oKO group, based on KEGG analysis of paracrine pathway genes. This up-regulation has been documented to lead to abnormal aggravation of inflammation within the cartilage layer in arthritis, and induced apoptosis. Additionally, its KO within chondrocytes lowered chondrocyte hypertrophy (Ho et al., 2009; Wei and Li, 2015; Ushakov et al., 2020). All of this was consistent with our findings of increased chondrocyte apoptosis and hypertrophic cartilage in oKO.

5. Conclusions

In this study, a FAM20C conditional KO mouse model, in which FAM20C was deleted from pre-osteoblasts, was established. Lower bone tissue mineralization and trabecular formation was observed, as well as increased cartilage hypertrophic layer thickness and apoptotic chondrocytes. These phenomena were found to be associated with up-regulation of genes promoting osteoclast differentiation and activity, such as *Sirpb1a-c* and *Mapk1*, along with down-regulation of osteogenesis-related genes, such as *Osx*, *Alp*, *Ocn*, *Mepe*, and *Col2*. Therefore, FAM20C KO resulted in abnormal long bone development; suggesting that manipulation of FAM20C activity could serve as a potential therapeutic target for treating bone disease and aging-related degeneration. Future studies, though, are required to pinpoint the causative pathways linking FAM20C to bone development.

Funding

This work was supported by the National Natural Science Foundation of China (Grant Nos. 81801040, 81870736, 81500816, 81570951) and Natural Science Foundation of Heilongjiang Province of China (LH2020H057).

CRedit author contribution statement

Lili Jiang: Conceptualization, Methodology, Validation, Formal analysis, Writing-Original Draft. **Xinpeng Liu:** Formal analysis, Writing-Original Draft, Project administration. **Lixue Liu:** Investigation, Resources, Data Curation, Visualization. **Lide Su:** Formal analysis, Writing-Original Draft, Project administration. **Zeyu Lu:** Investigation,

Resources, Data Curation. **Hong Zhang:** Investigation, Resources, Data Curation,. **Yuyao Guo:** Data Curation, Visualization. **Wenxuan Zhang:** Data Curation, Visualization. **Shujian Zhang:** Resources, Data Curation. **Wenxia Xu:** Investigation, Data Curation. **Jiahui Zhang:** Investigation, Resources. **Kai Zhang:** Investigation, Resources. **Yuanbo Zhan:** Writing-Review & Editing. **Xiaohua Xie:** Writing-Review & Editing. **Runhang Li:** Investigation. **Xinhe Dong:** Investigation. **Han Jin:** Writing-Review & Editing. **Bin Zhang:** Project Administration, Funding acquisition, Supervision. **Ying Li:** Project Administration, Funding acquisition, Supervision.

Declaration of Competing Interest

The authors declare no conflict of interest.

Data availability

Data will be made available on request.

Ethics approval

All animal procedures were approved by the Ethics Committee of Second Affiliated Hospital of Harbin Medical University (REB #: SYDW2021-079), and were carried out in accordance with the Guide for the Care and Use of Laboratory Animals (NIH, 8th Edition, 2011).

Acknowledgments

We thank Dr. Qin Chun Lin's research team for the donation of the FAM20C^{flox/flox} mouse, Dr. Yao Sun's research team for the donation of the Osx-Cre mouse, and Alina Yao for her assistance in manuscript preparation and editing.

Appendix A. Supplementary data

Supplementary data to this article can be found online at

References

- Barclay, A.N., 2016. A Comprehensive Review of Immunoreceptor Source Clin Rev Allergy Immunol. 50, 48-58.
- Barclay, A.N. and Brown, M.H., 2006. The SIRP family of receptors and immune regulation. Nature Reviews Immunology 6, 457-464.
- Beek, E.M., Vries, T.J., Mulder, L., Schoenmaker, T., Hoeben, K.A., Matozaki, T., Langenbach, G.E.J., Kraal, G., Everts, V. and Berg, T.K., 2009. Inhibitory regulation of osteoclast bone resorption by signal regulatory protein α . The FASEB Journal 23, 4081-4090.
- Berendsen, A.D. and Olsen, B.R., 2015. Bone development. Bone 80, 14-18.
- Da, Q., Han, H., Valladolid, C., Fernández, M., Khatlani, T., Pradhan, S., Nolasco, J., Matsunami, R.K., Engler, D.A., Cruz, M.A. and Vijayan, K.V., 2019. In vitro phosphorylation of von Willebrand factor by FAM20c enhances its ability to support platelet adhesion. Journal of Thrombosis and Haemostasis 17, 866-877.
- Dab, S., Abdelhay, N., Figueredo, C.A., Ganatra, S. and Gibson, M.P., 2022. Characterization of SIBLING Proteins in the Mineralized Tissues. Dentistry Journal 10.
- Dai, J., 2020. Osteoclast-derived exosomal let-7a-5p targets Smad2 to promote the hypertrophic differentiation of chondrocytes. American Journal of Physiology 1, 319.
- Dietrich, J., 2000. Cutting edge: signal-regulatory protein beta 1 is a DAP12-associated activating receptor expressed in myeloid cells. Journal of immunology. 164.
- Dzamukova, M., Brunner, T.M., Miotla-Zarebska, J., Heinrich, F., Brylka, L., Mashreghi, M.-F., Kusumbe, A., Kühn, R., Schinke, T., Vincent, T.L. and Löhning, M., 2022. Mechanical forces couple bone matrix mineralization with inhibition of angiogenesis to limit adolescent bone growth. Nature Communications 13.
- Geng, Y.-W., Zhang, Z., Jin, H., Da, J.-L., Zhang, K., Wang, J.-Q., Guo, Y.-Y., Zhang, B. and Li, Y., 2022. Mesenchymal-to-epithelial transition of osteoblasts induced by Fam20c knockout. Genes & Genomics 44, 155-164.
- Gibson, M.P., Zhu, Q., Wang, S., Liu, Q., Liu, Y., Wang, X., Yuan, B., Ruest, L.B., Feng, J.Q., D'Souza, R.N., Qin, C. and Lu, Y., 2013. The Rescue of Dentin Matrix Protein 1 (DMP1)-deficient Tooth Defects by the Transgenic Expression of Dentin Sialophosphoprotein (DSPP) Indicates That DSPP Is a Downstream Effector Molecule of DMP1 in Dentinogenesis. Journal of Biological Chemistry 288, 7204-7214.
- Graef, J.L., 2017. Osteoclast Differentiation is Downregulated by Select Polyphenolic Fractions from Dried Plum via Suppression of MAPKs and Nfatc1 in MouseC57BL/6 Primary Bone Marrow Cells. CURRENT DEVELOPMENTS IN NUTRITION 1.
- Hayashi, A., 2004. Positive Regulation of Phagocytosis by SIRP β and Its Signaling Mechanism in Macrophages. 279, 299450-60.

- Hayman, A.R., 2008. Tartrate resistant acid phosphatase Source Autoimmunity. 41.
- Hirose, K., Ishimoto, T., Usami, Y., Sato, S., Oya, K., Nakano, T., Komori, T. and Toyosawa, S., 2020. Overexpression of Fam20C in osteoblast in vivo leads to increased cortical bone formation and osteoclastic bone resorption. *Bone* 138.
- Ho, L., Stojanovski, A., Whetstone, H., Wei, Q.X., Mau, E., Wunder, J.S. and Alman, B., 2009. Gli2 and p53 Cooperate to Regulate IGFBP-3-Mediated Chondrocyte Apoptosis in the Progression from Benign to Malignant Cartilage Tumors. *Cancer Cell* 16, 126-136.
- Kim, J.-M., Lin, C., Stavre, Z., Greenblatt, M.B. and Shim, J.-H., 2020. Osteoblast-Osteoclast Communication and Bone Homeostasis. *Cells* 9.
- Liu, C., Zhang, H., Jani, P., Wang, X., Lu, Y., Li, N., Xiao, J. and Qin, C., 2017a. FAM20C regulates osteoblast behaviors and intracellular signaling pathways in a cell-autonomous manner. *Journal of Cellular Physiology* 233, 3476-3486.
- Liu, J., Saiyin, W., Xie, X., Mao, L. and Li, L., 2020. Ablation of Fam20c causes amelogenesis imperfecta via inhibiting Smad dependent BMP signaling pathway. *Biology Direct* 15.
- Liu, P., Ma, S., Zhang, H., Liu, C., Lu, Y., Chen, L. and Qin, C., 2017b. Specific ablation of mouse Fam20C in cells expressing type I collagen leads to skeletal defects and hypophosphatemia. *Scientific Reports* 7.
- Liu, X., Jiang, L., Zhang, W., Zhang, J., Luan, X., Zhan, Y., Wang, T., Da, J., Liu, L., Zhang, S., Guo, Y., Zhang, K., Wang, Z., Miao, N., Xie, X., Liu, P., Li, Y., jin, H. and Zhang, B., 2023. Fam20c regulates the calpain proteolysis system through phosphorylating Calpasatatin to maintain cell homeostasis. *Journal of Translational Medicine* 21.
- Palma-Lara, I., Pérez-Ramírez, M., García Alonso-Themann, P., Espinosa-García, A.M., Godinez-Aguilar, R., Bonilla-Delgado, J., López-Ornelas, A., Victoria-Acosta, G., Olguín-García, M.G., Moreno, J. and Palacios-Reyes, C., 2021. FAM20C Overview: Classic and Novel Targets, Pathogenic Variants and Raine Syndrome Phenotypes. *International Journal of Molecular Sciences* 22.
- Romeo, S.G., Alawi, K.M., Rodrigues, J., Singh, A., Kusumbe, A.P. and Ramasamy, S.K., 2019. Endothelial proteolytic activity and interaction with non-resorbing osteoclasts mediate bone elongation. *Nature Cell Biology* 21, 430-441.
- Ruhl, T. and Beier, J.P., 2019. Quantification of chondrogenic differentiation in monolayer cultures of mesenchymal stromal cells. *Analytical Biochemistry* 582.
- Salhotra, A., Shah, H.N., Levi, B. and Longaker, M.T., 2020. Mechanisms of bone development and repair. *Nature Reviews Molecular Cell Biology* 21, 696-711.

- Sundaram, K., Sambandam, Y., Shanmugarajan, S., Rao, D.S. and Reddy, S.V., 2017. Measles virus nucleocapsid protein modulates the Signal Regulatory Protein- β 1 (SIRP β 1) to enhance osteoclast differentiation in Paget's disease of bone. *Bone Reports* 7, 26-32.
- Tagliabracci, V.S., Wiley, S.E., Guo, X., Kinch, L.N., Durrant, E., Wen, J., Xiao, J., Cui, J., Nguyen, K.B., Engel, J.L., Coon, J.J., Grishin, N., Pinna, L.A., Pagliarini, D.J. and Dixon, J.E., 2015. A Single Kinase Generates the Majority of the Secreted Phosphoproteome. *Cell* 161, 1619-32.
- Tomasello, E., 2015. Association of signal-regulatory proteins beta with KARAP/DAP-12. *European Journal of Immunology* 30.
- Udagawa, N., Koide, M., Nakamura, M., Nakamichi, Y., Yamashita, T., Uehara, S., Kobayashi, Y., Furuya, Y., Yasuda, H., Fukuda, C. and Tsuda, E., 2020. Osteoclast differentiation by RANKL and OPG signaling pathways. *Journal of Bone and Mineral Metabolism* 39, 19-26.
- Ushakov, R.E., Skvortsova, E.V., Vitte, M.A., Vassilieva, I.O., Shatrova, A.N., Kotova, A.V., Kenis, V.M. and Burova, E.B., 2020. Chondrogenic differentiation followed IGFBP3 loss in human endometrial mesenchymal stem cells. *Biochemical and Biophysical Research Communications* 531, 133-139.
- van Driel, M. and van Leeuwen, J.P.T.M., 2023. Vitamin D and Bone: A Story of Endocrine and Auto/Paracrine Action in Osteoblasts. *Nutrients* 15.
- van Gastel, N. and Carmeliet, G., 2021. Metabolic regulation of skeletal cell fate and function in physiology and disease. *Nature Metabolism* 3, 11-20.
- Wang, X., 2012. Inactivation of a Novel FGF23 Regulator, FAM20C, Leads to Hypophosphatemic Rickets in Mice. 8.
- Wei, Z. and Li, H.-H., 2015. IGFBP-3 may trigger osteoarthritis by inducing apoptosis of chondrocytes through Nur77 translocation 2015 8 12 15599 610.pdf>. 8, 15599-610.
- Xing, W., Godwin, C., Pourteymoor, S. and Mohan, S., 2019. Conditional disruption of the osterix gene in chondrocytes during early postnatal growth impairs secondary ossification in the mouse tibial epiphysis. *Bone Research* 7.
- Xu, R., Tan, H., Zhang, J., Yuan, Z., Xie, Q. and Zhang, L., 2021. Fam20C in Human Diseases: Emerging Biological Functions and Therapeutic Implications. *Frontiers in Molecular Biosciences* 8.
- Yao, Y., Cai, X., Ren, F., Ye, Y., Wang, F., Zheng, C., Qian, Y. and Zhang, M., 2021. The Macrophage-Osteoclast Axis in Osteoimmunity and Osteo-Related Diseases. *Frontiers in Immunology* 12.

- Yu, S., Guo, J., Sun, Z., Lin, C., Tao, H., Zhang, Q., Cui, Y., Zuo, H., Lin, Y., Chen, S., Liu, H. and Chen, Z., 2021. BMP2-dependent gene regulatory network analysis reveals Klf4 as a novel transcription factor of osteoblast differentiation. *Cell Death & Disease* 12.
- Zhang, H., Li, L., Kesterke, Matthew J., Lu, Y. and Qin, C., 2019. High-Phosphate Diet Improved the Skeletal Development of *Fam20c*-Deficient Mice. *Cells Tissues Organs* 208, 25-36.
- Zhang, H., Lu, Y., Kramer, P.R., Benson, M.D., Cheng, Y.-S.L. and Qin, C., 2023. Intracranial calcification in *Fam20c*-deficient mice recapitulates human Raine syndrome. *Neuroscience Letters* 802.
- Zhang, H., Zhu, Q., Cui, J., Wang, Y., Chen, M.J., Guo, X., Tagliabracci, V.S., Dixon, J.E. and Xiao, J., 2018. Structure and evolution of the *Fam20* kinases. *Nature Communications* 9.
- Zou, W., Zhu, T., Craft, C.S., Broekelmann, T.J., Mecham, R.P. and Teitelbaum, S.L., 2010. Cytoskeletal dysfunction dominates in *DAP12*-deficient osteoclasts. *Journal of Cell Science* 123, 2955-2963.
- Zuo, H., Yang, D. and Wan, Y., 2021. *Fam20C* Regulates Bone Resorption and Breast Cancer Bone Metastasis through Osteopontin and BMP4. *Cancer Research* 81, 5242-5254.

Figure Legends

Fig. 1. Osterix (Osx)-Cre; FAM20C^{lox/lox} knockout (oKO) mice had slower bone growth and poorer formation compared to FAM20C^{lox/lox} (control). (A) Mouse body weight growth curve, from 1-10 weeks, for oKO and control mice. (B) Whole-body lateral and (C) lower limb bone X-rays for the 2 mouse types, at 4-weeks-old. Yellow arrow represents the 2nd ossification center, and red arrow the epiphyseal plate area, in (C). (D) 3-dimensional (3D) reconstruction of 4-week-old mouse femur, based on micro-computed tomography (CT). Blue arrow represents cortical bone, yellow arrow the trabecular bone area at the distal end of the epiphyseal plate, and red arrow the epiphyseal plate. (E) Micro-CT of trabecular bone from the distal region of the epiphyseal plate of 4-week-old mice. (F) Osteometry results for bone trabeculae from the distal region of the epiphyseal plate, for 4-week-old mice. n=3/group for all experiments. ns=no statistical difference, *P<0.05; ***P<0.001.

Fig. 2. oKO mice demonstrated growth plate hypertrophy, thickened cartilage layer, and bone dysplasia. (A) Hematoxylin & eosin (H&E) staining images of the proximal femur from 4-week-old control and oKO mice. Black arrow represent the cell layers within the resting area of the cartilage, blue arrow the cartilage proliferation area, red arrow the cartilage hypertrophy area, and red star the articular cartilage hypertrophy area. (B) Safranin O-fast green staining for chondrocytes (red) in the epiphyseal region from 4-week-old mice. (C) TUNEL staining and (D) quantification for apoptotic cells. (E) Immunohistochemical staining and (F) quantification of cells positive for the apoptotic marker caspase-3 among epiphyseal tissue, at 4 weeks. Black arrow represents cartilage calcification, and red arrow

cartilage proliferation areas, with increased apoptosis in these 2 regions, for (C) and (E). n=3/group for all experiments. *P<0.05; **P<0.01.

Fig. 3. Transcriptome analysis results for femurs from oKO and control mouse groups.

(A) Number of differentially-expressed genes (DEGs) in oKO versus control groups. (B) Heat map showing DEG clustering. (C) Volcano plot showing up-regulated and down-regulated DEGs. (D) Bubble plot showing Gene Ontology (GO) enrichment results. (E) Bubble plot for Kyoto Genes and Genomes (KEGG) pathway enrichment results. n=3/group for all experiments.

Fig. 4. Knocking out FAM20C promoted osteoclast differentiation and suppressed osteogenesis.

(A) Tartrate-resistant acid phosphatase (TRAP) staining for osteoclasts within the femurs of 4-week-old mice, in control and oKO groups. Black arrow indicated multinucleated osteoclasts in the bone trabecula, and mononuclear osteoclasts in the ossification zone. (B) Osteoclast counts between the 2 mouse groups. Quantitative real-time PCR (qPCR) results, representing expression levels for (C) osteoclast-specific genes cathepsin K (Ctsk), matrix metalloproteinase protein 9 (Mmp9), nuclear factor of activated T-cells, cytoplasmic 1 (Nfatc1), and Trap, (D) osteoclast differentiation-associated genes signal regulatory protein β -1 family (Sirpb1a-c) and mitogen-activated protein kinase 13 (Mapk13), plus (E) osteogenesis-related genes Sp7 (Osx), alkaline phosphatase (Alp), osteocalcin (Ocn), matrix extracellular phosphoglycoprotein (Mepe), and collagen type 2 (Col2). n=3/group for all experiments. ns=no statistical difference, *P<0.05; **P<0.01; ***P<0.001.

Declaration of competing interest

The authors declare no conflict of interest.

Figure 1

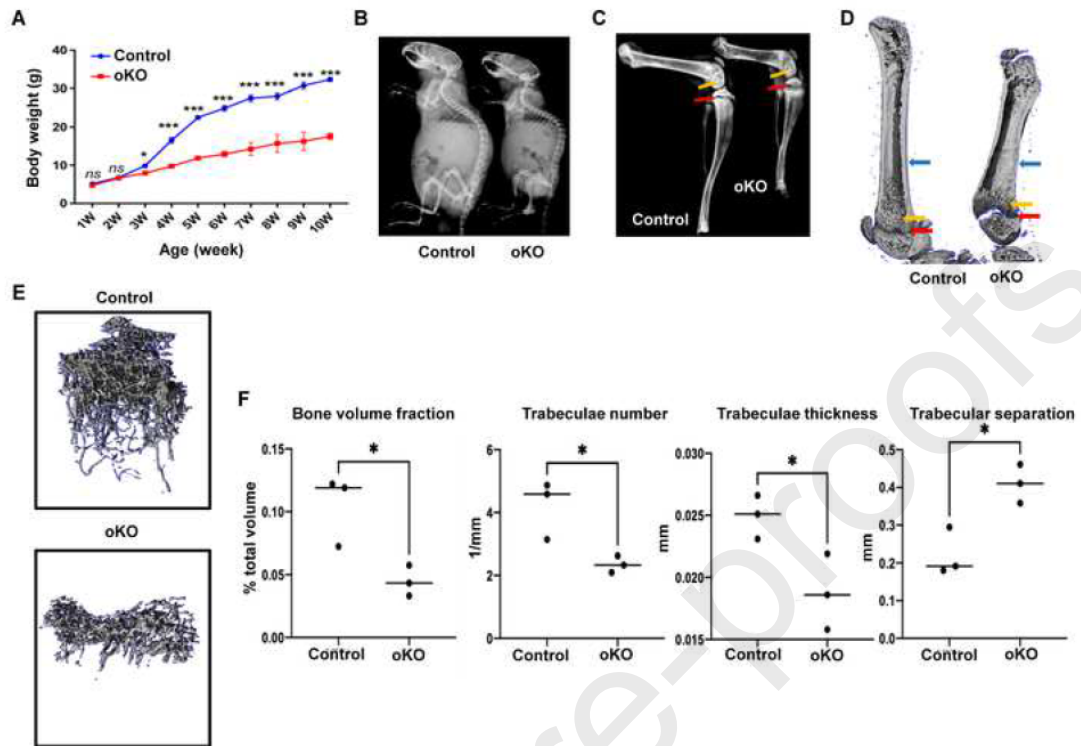
[Click here to access/download;Figure\(s\);Figure 1.tif](#)

Figure 2

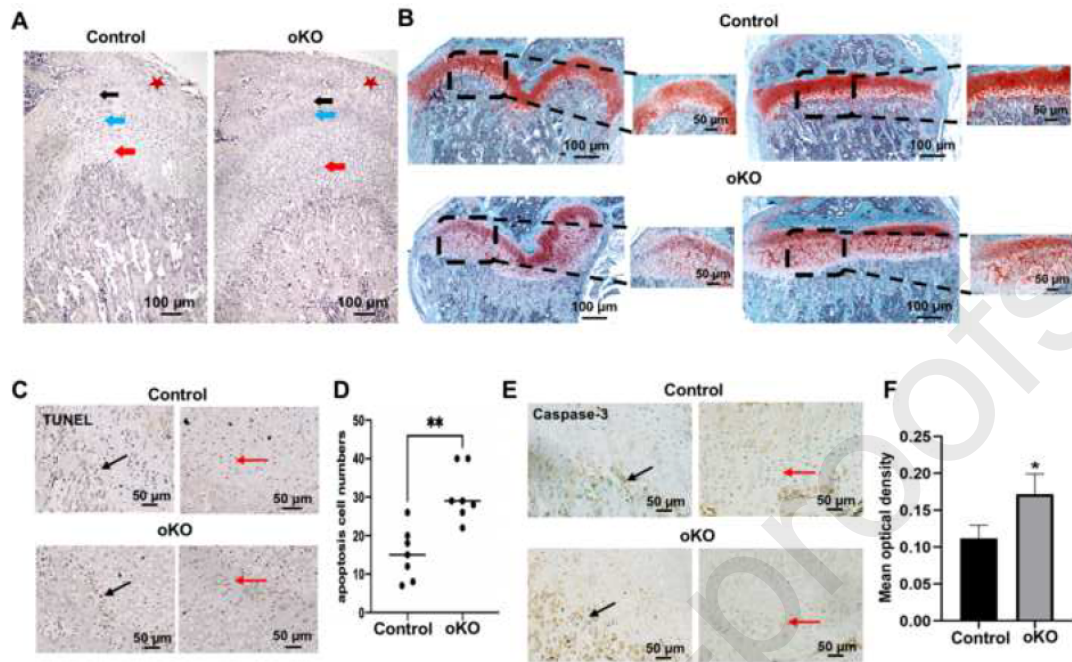
[Click here to access/download;Figure\(s\);Figure 2.tif](#)

Figure 3

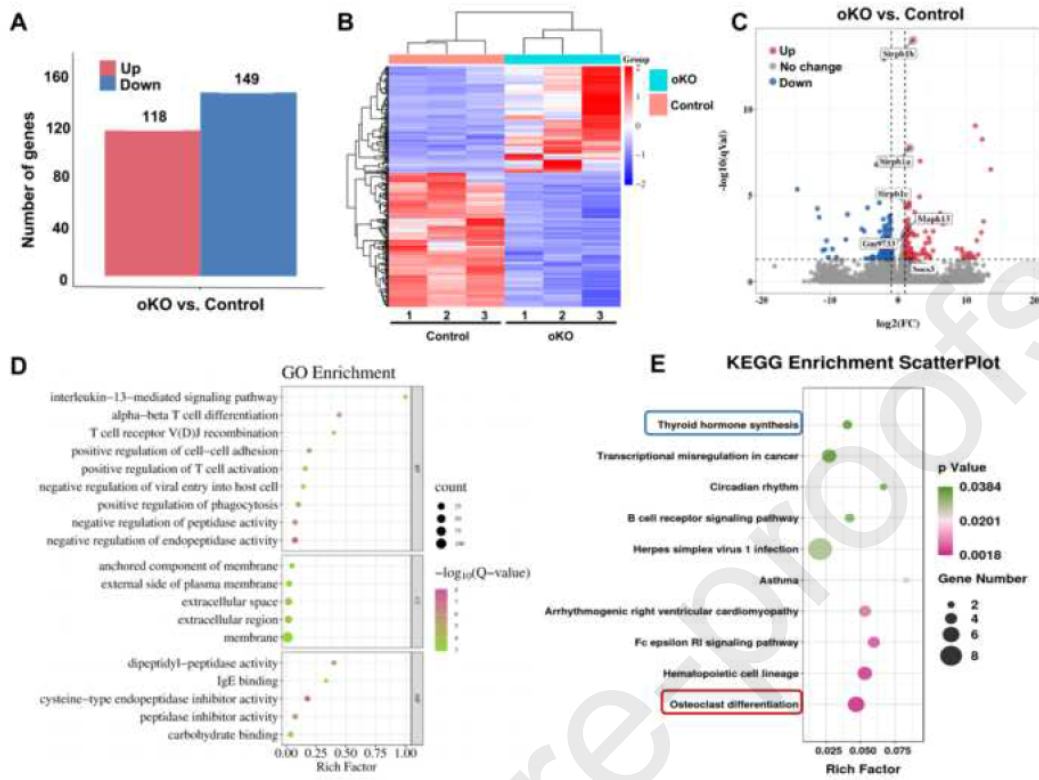
[Click here to access/download;Figure\(s\);Figure 3.tif](#)

Figure 4

[Click here to access/download;Figure\(s\);Figure 4.tif](#)